50th AIAA/ASME/ASCE/AHS/ASC Structures, Structural Dynamics, and Materials Conference
17th
4 - 7 May 2009, Palm Springs, California

AIAA 2009-2157

Rigidizable Inflatable Get-Away-Special Experiment (RIGEX) Space Flight Data Analysis

Brett J. Cooper[1], Jonathan T. Black[2], Eric D. Swenson[3], and Richard G. Cobb[4]
Air Force Institute of Technology, Wright-Patterson AFB, Ohio, 45433

The Rigidizable Inflatable Get-Away-Special EXperiment (RIGEX) was run successfully on board STS-123 (*Endeavor*) in March 2008. RIGEX was built by graduate students at the Air Force Institute of Technology (AFIT) and returned there following the shuttle flight for post-flight analysis. The experiment's objectives were to demonstrate in space the stowage, deployment, and rigidization techniques of carbon fiber composite inflatable rigidizable cylindrical booms. RIGEX was a Canister For All Payloads (CAPE) Space Shuttle cargo bay experiment designed to heat and inflate three 50.8 cm (20 in) long carbon fiber composite booms in a microgravity vacuum environment and measure both the structural characteristics and the deployment accuracy. Pressure, temperature, modal response, and position data were collected successfully on-orbit and are compared here to ground test data. This research is intended to help demonstrate the feasibility of using lightweight and low stowage volume (high packaging ratio) inflatable/rigidizable space structures for space mission applications.

I. Introduction

INFLATABLE space structures have long been acknowledged as a means of reducing complexity, weight, volume, and cost of large space systems. Beginning with the limited launch capabilities of the early space program, inflatable structures were used successfully in orbit multiple times.[1] Lack of understanding of the deployment processes in space coupled with large increases in space lift capacity led to the early space community to use more familiar metal structures. Spacecraft complexity has increased with increasing demands levied on space systems' performance, which drives increases in spacecraft weight and volume. It can be shown that increasing weight and volume increases overall spacecraft cost and launch cost, while limiting the potential number of space lift providers.[2]

As in the early space program, inflatable structures are again being investigated to reduce spacecraft weight, volume, and cost. As before, inflatable space structures still present many challenges, such as maintaining internal pressure for structural integrity. Though recent inflatable space experiments have lasted several years[3] without mission ending pressure loss events, it is conceivable that pressure loss could weaken the entire structure, possibly ending the mission. For a purely inflatable structure – one without any rigid components – there are few means to combat this limitation. An alternative to continual pressurization is to rigidize the structure after inflation.

Currently, the majority of the work associated with inflatable/rigidizable space structures has been confined to computer modeling and ground testing of deployment and structural characteristics.[4] The overall objective of RIGEX was to validate deployment and rigidization techniques for three 50.8 cm (20 inch) long carbon fiber tubes supplied by L'Garde Inc. in a microgravity environment and measure their rigidized structural and physical characteristics for correlation with ground test data. The recent space test was a successful proof of concept demonstration, and will result in a Technology Readiness Level (TRL) increase for the future DoD use of inflatable/rigidizable technology to help alleviate payload mass and volume limitations.

---

[1] Captain, USAF, Student, Dept. of Aeronautics and Astronautics, 2950 Hobson Way, AIAA Student Member.
[2] Assistant Professor, Dept. of Aeronautics and Astronautics, 2950 Hobson Way, AIAA Member.
[3] Lt Col, USAF, Assistant Professor, Dept. of Aeronautics and Astronautics, 2950 Hobson Way, AIAA Member.
[4] Assistant Professor, Dept. of Aeronautics and Astronautics, 2950 Hobson Way, AIAA Associate Fellow.

II. Experiment Description

RIGEX was an experiment designed to be mounted inside the CAPE canister attached to the rear of Space Shuttle cargo bay (Fig. 1). This location allowed the experiment to draw power from the shuttle for testing purposes while being exposed to the ambient space vacuum, temperature, and microgravity. The experiment was cylindrical as specified by the NASA CAPE payload envelope. NASA limits overall experiment weight to 159 kg, and size to 53 cm in diameter and 135 cm in height.

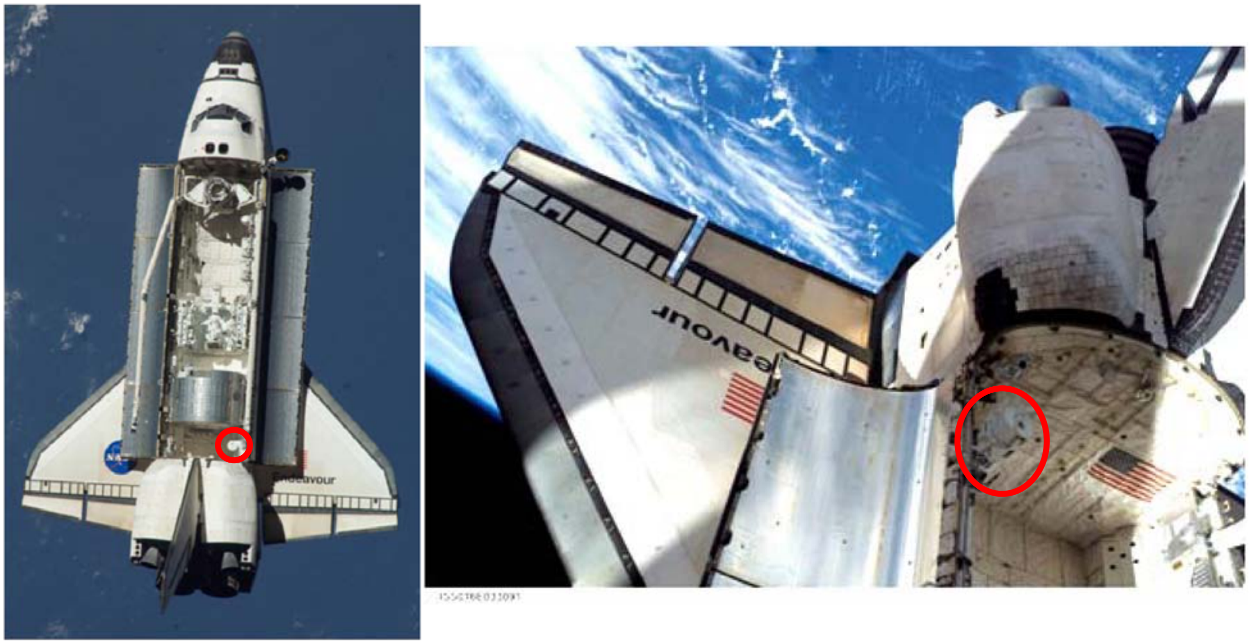

Fig. 1 RIGEX in *Endeavour* (STS-123) cargo bay highlighted by red circle.

The RIGEX experiment consisted of three tube (boom) bays and a computer bay, arranged radially about an open center which stored the pressure tanks for inflation. Figure 2 shows a Computer Aided Drawing (CAD) representation of RIGEX. Immediately visible are two inflatable/rigidizable tube bays; the right bay shows an inflated and rigidized boom rising out of an unlatched oven box, and the left bay shows a stowed boom. The bottom of the representation shows the tubing required for the inflation events, above the booms are cameras, and attached to the tip of the boom are the accelerometers.

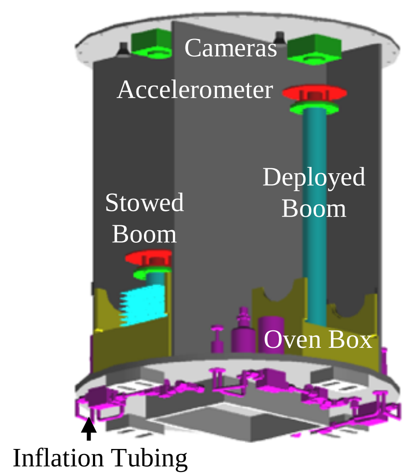

Fig. 2 CAD representation showing tube bays.

The inflatable, rigidizable tubes were manufactured by L'Garde, Inc. and consist of a three ply carbon fiber layup and a proprietary thermoplastic resin based on a polyurethane elastomer. The material is designed to transition from rigid to pliable at a glass transition temperature of 125°C. RIGEX used resistive heaters to heat the folded tubes through the transition temperature, at which point the ovens turned off and unlatched, allowing the tubes to deploy. Residual strain energy stored during the stowing process deployed the tube slightly upon release of the oven latches, at which point nitrogen was injected into the tubes, bringing them to fully deployed configurations. After inflation, the tubes cooled below the transition temperature, rigidized, and vented the nitrogen. The tubes were then excited by attached macro fiber composite (MFC) piezoelectric patches supplied by NASA Langley Research Center for vibration response testing.

Aside from external power from the shuttle, RIGEX was a wholly self-contained experiment. Power was required for the computer, ovens, cameras, light emitting diodes (LEDs), MFC patches, and accelerometers. The Shuttle provided RIGEX with a maximum of 14.25 amps for the resistive heaters. While in space, the only interface with RIGEX was an on-off toggle switch and display indicator on the Standard Switch Panel accessible to the astronauts in the middeck. The experiment therefore ran autonomously from start to finish.

III. Data Collection

The RIGEX data collection activities are divided into those that occurred during the Shuttle flight, during and after boom deployment, and those that occurred after the flight at AFIT. The deployment phase collections occurred on orbit during the physical process necessary to deploy the booms from their stowed configurations. The post deployment data collections occurred during the vibration response testing conducted immediately after the deployment. The post flight data collections occurred after the experiment was removed from *Endeavor* and returned to AFIT.

RIGEX was activated during quiescent operations on Flight Day 14 (24 March 2008) of STS-123. Pressure and temperature data were collected during boom deployment, and acceleration data was collected post boom deployment. Post flight data collected at AFIT consists of precise three dimensional (3D) physical alignment measurements of the deployed tubes and further vibration testing of the deployed tubes using higher fidelity ground test hardware.

A. Deployment

The deployment phase began with an astronaut toggling the RIGEX power switch on the Standard Switch Panel to “On,” which supplied power to the experiment. Upon receiving power, the computer automatically booted up and ran through a variety of memory verifications. Then the thermocouples attached to the computer board and base of the experiment structure were activated. After recording the pressure of the nitrogen storage tanks, the computer turned on the resistive heater oven in Bay 1, which began radiating heat and warming the tube. LEDs illuminated the bay, and the camera at the top of the bay collected images every 50 seconds. Two thermocouples mounted inside the tube folds recorded the tube temperature, and after the tubes warmed sufficiently above the glass transition temperature of 125°C the accelerometers at the top of the tubes activated and the oven door latch released, springing the doors open. After the oven doors opened, pressure transducers began to monitor pressure inside of the valve connecting the boom to the nitrogen storage tank which then opened, and nitrogen filled the tube. The pressure equalized after the tube completely inflated in less than ten seconds, and pressure and acceleration recordings ended five seconds after they began. The camera stopped taking pictures, the LEDs turned off, and thermocouple temperature data stopped being recorded. After a five minute hold to allow the boom to cool and rigidize, the inflation valve was moved to the vent position, venting the tube to ambient, and concluding the deployment test phase for tube 1. The same process was utilized for the next two tubes, as shown in Fig. 3. Fig. 4 shows a stowed tube z-folded folded for launch and a deployed tube, respectively.

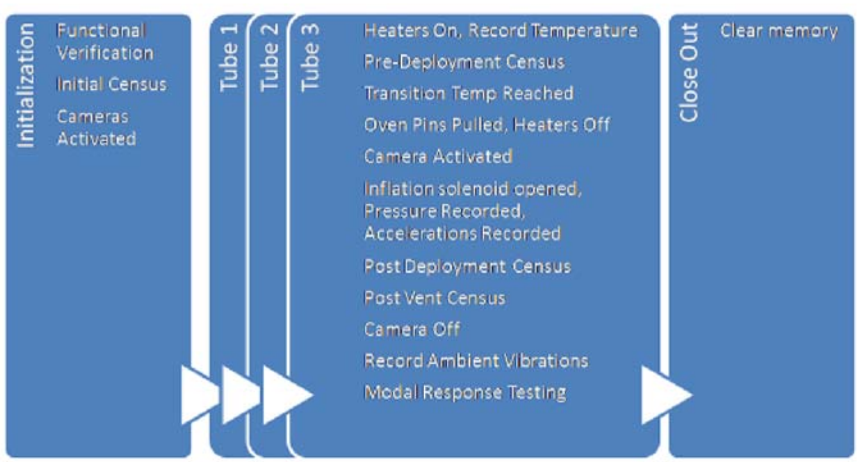

Fig. 3 RIGEX experiment timeline.

Fig. 4 Stowed and deployed RIGEX booms.

B. Post Deployment

The post deployment on-orbit data collection began after each tube had cooled and rigidized. This phase involved five minutes of forced vibration testing, using the attached MFC patches and accelerometers. A 0-2000 Hz chirp signal was sent to the MFC patches over a period of one second.

The vibration data sample rate was 5000 Hz. During each excitation event, the tube tip accelerometers monitored and recorded acceleration data. After 25 one-second excitation events were run on each tube, the post deployment phase was complete for that particular tube and the experiment moved to deployment phase for the next tube. After post deployment phase activities were complete for tube 3, the computer automatically shutdown and the astronauts toggled the power switch to "off." The total experiment time for RIGEX was approximately 70 minutes.

C. Post Flight

Post flight data collection activities are associated with all tests that occurred after the experiment had been offloaded from *Endeavor* following the flight and returned to AFIT. The orbital experimental data was copied at Cape Canaveral and the experiment was packed and shipped to AFIT. When RIGEX arrived at AFIT, it was unpacked and examined for any changes that may have occurred during shipment.

The first post flight data collection was a precision 3D physical alignment measurement, conducted with a FARO seven axis two-meter Platinum Arm with a hard probe. The measurements produce 3D point clouds which were then imported into 3D CAD models. The models then are compared to perfectly straight tube deployments and distance measurements are taken to determine deployment errors.

The next test was used to determine ground truth vibration response data for comparison to flight data, as well as previous vibration data from similar tubes. A 3D scanning laser vibrometer was used to measure the induced vibration response in the *x*-, *y*-, and *z*-directions. The signal analyzer/user interface software was used to align the laser heads and generate a grid of points to scan. Combining each scan point's response from all three vibrometer heads allows the system to measure 3D frequency response functions (FRFs) and animate the operating deflection shapes corresponding to peaks in the FRFs. The flight piezoelectric patches excited the tubes with externally-generated 0-500Hz and 0-5000Hz chirp signals. Fig. 5 shows the test setup.

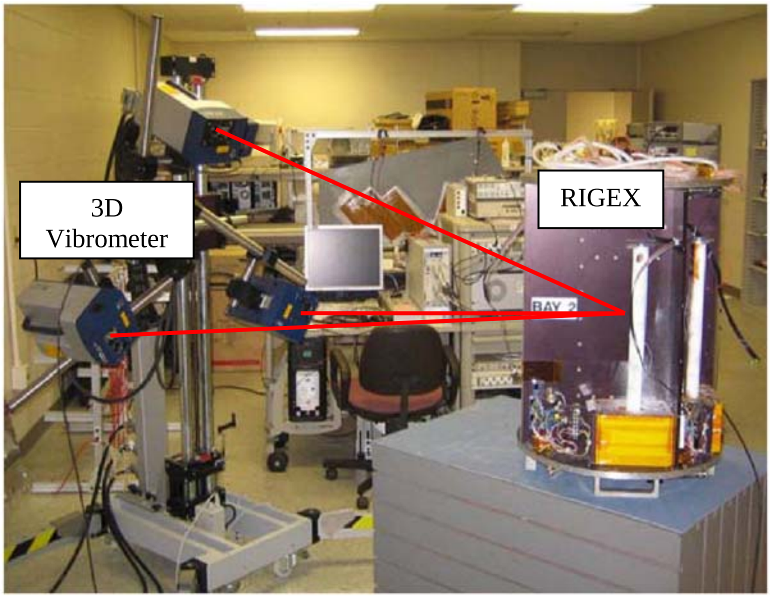

Fig. 5 Post flight 3D scanning laser vibrometer test setup.

Additional vibration response tests were conducted using accelerometers and a surrogate flight computer set up, but these tests merely confirmed the 3D laser vibrometer data and therefore are not presented here.

IV. RIGEX Test Results and Analysis

Analysis of the flight data began immediately after RIGEX was removed from *Endeavor*. The data was copied from the onboard computer and several pictures of the experiment and deployed tubes were taken, showing that the experiment was a success (Fig. 6). RIGEX was then shipped to AFIT, and for the next several months data analysis and post flight testing were conducted.

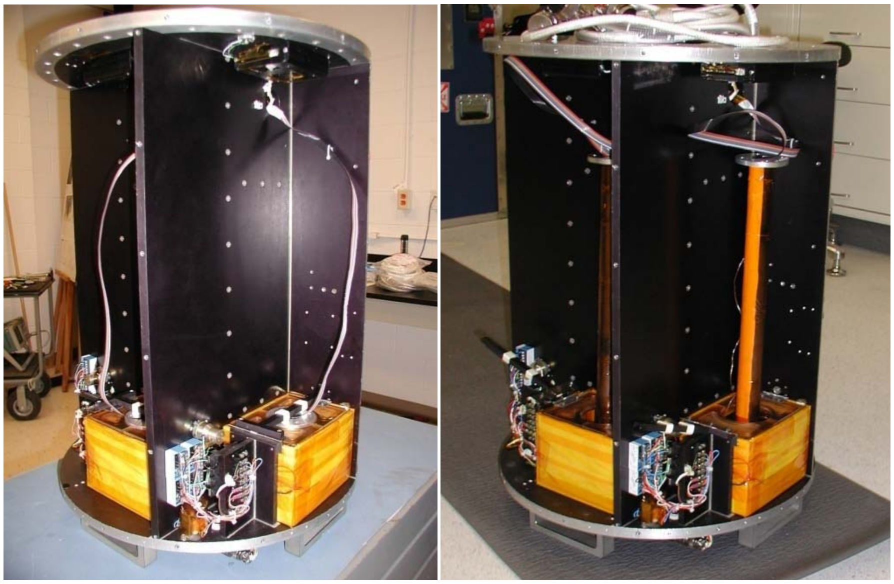

Fig. 6 RIGEX prior to shuttle integration (left) and following shuttle return (right)

A. Deployment

The on-orbit deployment phase test data can be broken into three categories: temperature data, pressure data, and accelerometer data. Fig. 7 is a collection of graphs that show the time history temperature data for all three boom heatings prior to inflation. Thermocouples measured temperature near one of the external folds of each stowed tube (Thermocouple A) and as close to the center of each tube boom as possible (Thermocouple B), in the experiment structure, and on the computer processor board. As expected, tube 1, the first tube to run in the experiment, started at the lowest temperature for all readings, followed by tube 2 and tube 3. After the experiment had cold soaked for 14 days on-orbit, the coldest temperature recorded was tube 1 thermocouple A at ~-35°C. Both the A and B thermocouples mounted to the tubes track along similar but slightly different paths. This trend is explained by the location of the thermocouples on the interior folds of the stowed tubes. Thermocouple A was more directly exposed to the resistive heaters and thus reads higher over time for all tubes, and also increases at a faster rate. Tube 2's folding pattern was different from the other two tubes, which may explain the deviation in heating rate from the other two tubes.

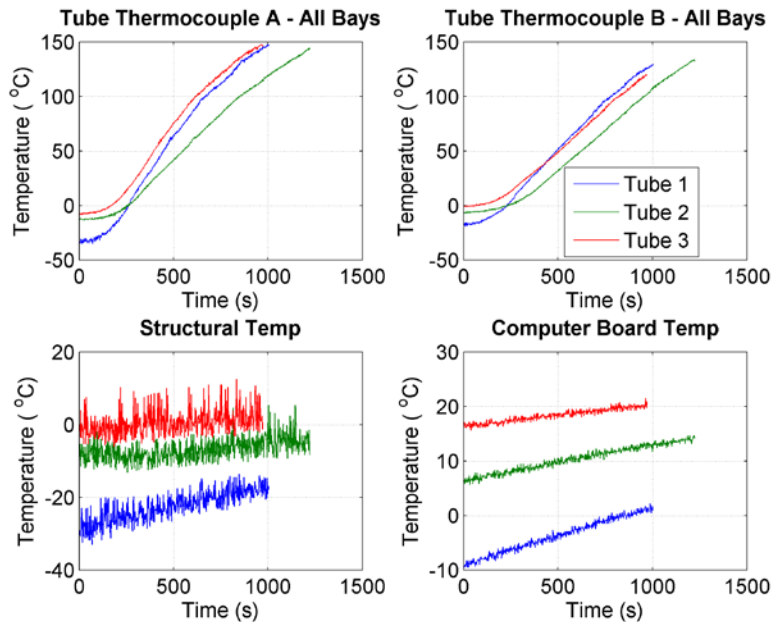

Fig. 7 Deployment temperature verse time for all thermocouple locations.

After the tube 1 deployment and post deployment data collections were complete, the tube 2 starting temperature was considerably higher due to the radiative and conductive heating effects of the oven operation. The structural thermocouple reading slope is much steeper for the tube 1 deployment than for the tube 2 and 3 deployments. This discrepancy seems to indicate the resistive heaters radiative and conductive heating effects on structural temperature taper off toward equilibrium as the structure reaches higher temperatures, however, the structural thermocouple placement was also closest to tube 1, which limits the radiative effects felt from tube 2 and 3 ovens. In reality, the slope change from tube to tube is probably caused by both increasing structural temperature and distance from the second and third oven.

The computer processor board thermocouple readings follow the same pattern as the structural thermocouple readings. During tube 1 deployment, the computer thermocouple starts at its lowest reading of ~-10°C and trends to 0°C over 1000 seconds. Tube 2 and 3 deployment readings start significantly higher (-3°C and 0°C, respectively), but trend at lower rates. Again, this is likely attributable to increased temperature reducing radiative heating efficiency and increasing oven distance from the thermocouple. The initial and final temperatures observed by the computer board thermocouple were 15-20°C higher than the structural initial and final temperature; this discrepancy is a result of the computer generating heat during operations.

Figure 8 graphically represents the data from the measured pressure inside of the tubes and accelerometer readouts during the inflation process. Immediately obvious is the lack of inflation pressure and substantial accelerations in tube 1 indicating that it did not inflate. It is believed the tube 1 inflation valve suffered from stiction during actuation, and did not open immediately when commanded. This is possibly attributable to the -20°C temperature of the structure at the time inflation was commanded. Post-flight inspection, however, shows that tube 1 did in fact inflate, though it is significantly less straight than the other two tubes, which indicates inflation probably occurred after the tube had cooled somewhat and became moderately stiff. Inflation did occur successfully, however, as pressure was measured in the tube after deployment and during the venting process (see Table 1).

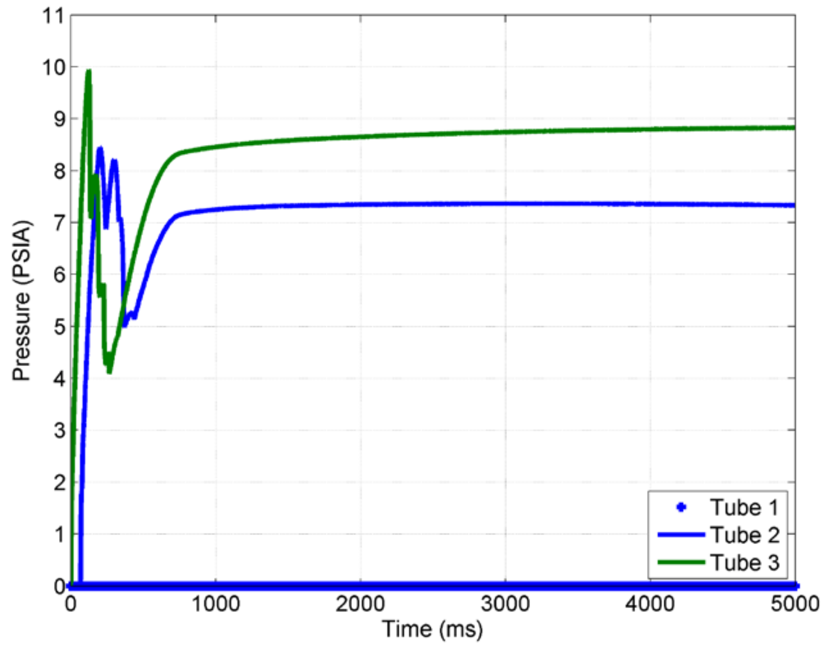

Fig. 8 Deployment pressure versus time for all three booms.

Tube 2 and 3 show similar characteristics with an initial and secondary pressure spike associated with straightening of folds. The pressure rapidly builds behind the first fold, spiking at 8 and 10 psia for tubes 2 and 3, before the pressure opens the fold enough to allow pressure to begin inflating the tube behind the first fold. At this point, the pressure builds again and pushes through the second fold. There are 6 folds in the stowed tubes (Fig. 4), four 180° folds and two partial folds (Figure 2). In both tube 2 and 3, there are four spikes in the pressure data, which correlate to pressure building behind each of the four 180° folds.

The three-axis accelerometer data for tubes 2 and 3 shown in Fig. 9 reinforces the inflation analysis above. Tube 2 does not read any acceleration in any direction until the pressure spikes and the inflation gas gets through the first and second folds. At that point, all three directions begin to show acceleration. Tube 3 accelerations were above the noise level immediately; the larger pressure spike most likely initiated motion earlier than tube 2, but the tube 3 acceleration spikes are not as distinguishable as the tube 2 acceleration spikes. As each tube deployed, the accelerometer's coordinate frame moved within inertial space; thus the *x*-, *y*-, and *z*-axis acceleration data is local to the aluminum end cap.

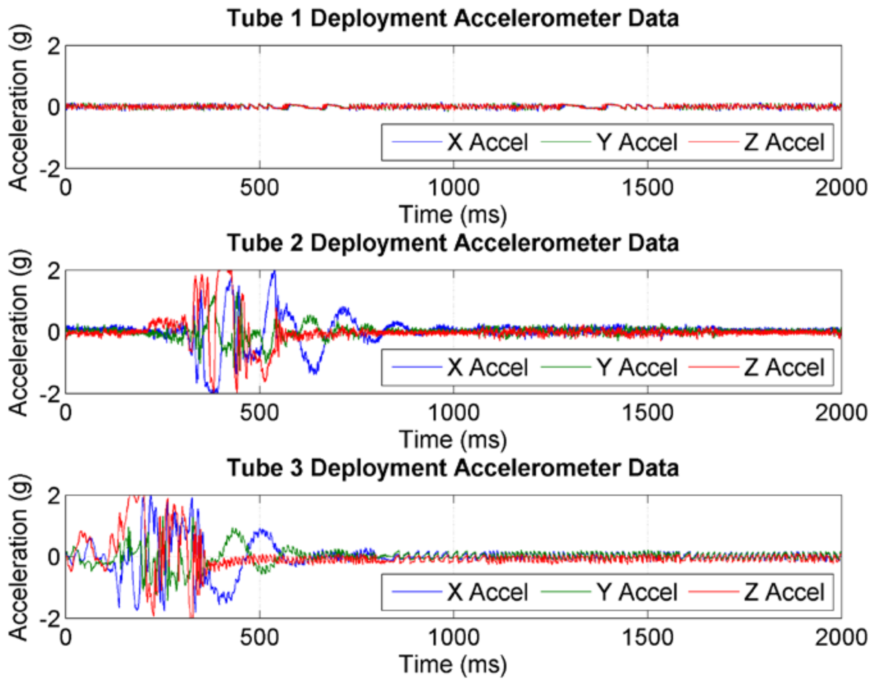

Fig. 9 Acceleration versus time for all three booms.

A slight delay is present in inflation pressure readings for tube 2, which is accompanied by a slightly longer delay in acceleration readings for tube 2. It is believed the tube 2 inflation valve also suffered from a brief bout of cold induced stiction, but rapidly recovered. The additional delay before accelerations were observed for tube 2 and the difference in inflation pressure profile (relative to tube 3) is potentially explained by a difference in tube 2's stowed *z*-fold configuration.

Table 1 provides pressure values for the supply tanks and the tubes at discrete points in the experiment timeline. The flight code was programmed to take pressure readings at experiment initialization and at important points in the tube deployment process. Several of the data attributes are immediately recognizable: tube pressure values prior to commanded inflation are 0 psia and return to 0 psia after commanded venting, the tube and tank pressures are approximately equal after the commanded inflation, tube 1 does register pressure after commanded inflation, tube 2 registers a much lower pressure after commanded inflation than tubes 1 & 3, and only tube 3 reads the same approximate value after inflation as Fig. 8 indicates.

Table 1 Discrete tank and tube pressures (psia) during experiment.

	Tank 1 Pressure	Tube 1 Pressure	Tank 2 Pressure	Tube 2 Pressure	Tank 3 Pressure	Tube 3 Pressure
Experiment Initialization	14.85	0.00	12.38	0.00	14.48	0.00
Tube 1 Initialize	14.83	0.00	12.37	0.00	14.46	0.00
Tube 1 Deploy + 300s	5.26	5.12	12.38	0.00	14.48	0.00
Tube 1 Vent + 5s	5.26	0.10	12.38	0.00	14.48	0.00
Tube 2 Initialize	5.26	0.00	12.39	0.00	14.49	0.00
Tube 2 Deploy + 300s	5.28	0.00	1.24	1.17	14.53	0.00
Tube 2 Vent + 5s	5.28	0.00	1.23	0.00	14.53	0.00
Tube 3 Initialize	5.28	0.00	1.23	0.00	14.55	0.00
Tube 3 Deploy + 300s	5.30	0.00	1.23	0.00	8.26	8.18
Tube 3 Vent + 5s	5.29	0.00	1.23	0.00	8.26	0.13

As discussed above, tube 1 did not inflate while the accelerometer and pressure transducer data were being collected, but there are pressure readings for tube 1 taken 300 seconds after commanded inflation. Unfortunately, there are no other pressure readings between commanded inflation +5 seconds and +300 seconds, so it is not clear as to when the tube inflated. Based on preflight vacuum chamber test results, tube cooling profiles indicate tube 1 probably inflated within 50 seconds of the inflation command. Any further delay would have likely resulted in improper deployment as the composite material cooled to its glass-transition temperature. Tubes 1 and 3 both read low pressure after venting was commanded. This indicates venting was mostly complete in 5 seconds.

Tank 2 started with 15% less pressure than the other tanks, and the equilibrium pressure 300 seconds after tube 3's commanded inflation was significantly less than tubes 1 and 3 equilibrium pressures (76 and 85%, respectively). It is thought that tube 2 leaked after inflation, which may be the explanation for its slightly decreasing pressure at the end of 5 seconds in Fig. 8, whereas tube 3 slowly increased in pressure. The last tube 2 pressure reading in Fig. 8 is 7.3323, much different from the 1.17 psia indicated in Table 1, whereas the last tube 3 pressure reading in Fig. 8 is 8.828 psia, very close to the 8.18 cited in Table 1. Tubes 2 and 3 differ by 1.5 psia at the end of Fig. 8.

Figures 10 and 11 show deployment images of tube1 and tube 2. These images are taken after the oven door has released and prior to inflation. Residual strain energy stored during boom stowage caused the tubes to push slightly out of the ovens. The LED's provided more than adequate illumination for the pictures, allowing the components to be easily distinguished. Note for tube 1, both oven doors appear to be pushed open, but tube 2 only pushes the right oven door open. These figures give us insight into how the tubes physically deploy in a microgravity environment. The maximum frame rate for the camera was 0.9 seconds, so only one photo of the deployment process exists for the tubes.

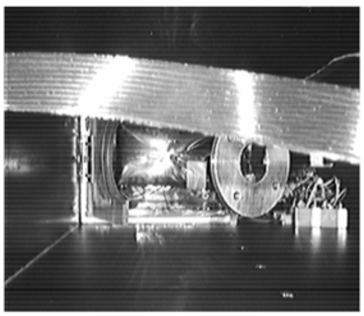

Fig. 10 Tube 1 inflation deployment photo.

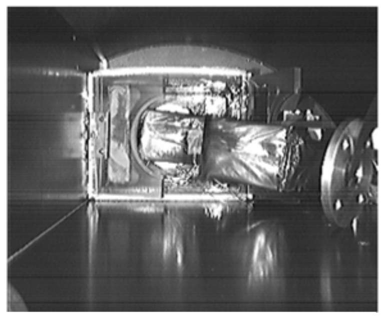

Fig. 11 Tube 2 inflation deployment photo.

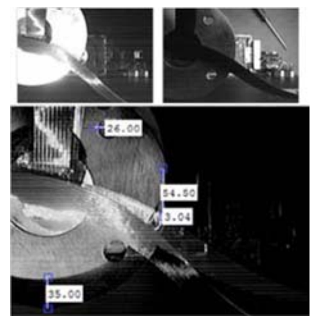

Fig. 12 On-orbit, post flight, and composite image.

The images were further analyzed using MATLAB® image processing tools. Fig. 12 shows an on-orbit and post flight image of deployed tube 3 and a composite image resulting from subtracting intensities of the two. By subtracting intensities, the physical change in the tube endcap position from the on-orbit image to the post flight image can be determined. This measurement of relative change in position can then be combined with precision ground-based knowledge to determine on-orbit deployment accuracy, which is discussed later. Unfortunately, the camera for tube 2 was inoperable upon return to AFIT, so no post flight images are available for tube 2.

B. Post Deployment

The post deployment phase test results focused on the on-orbit vibration response of the deployed tubes. At first, analysis of the on-orbit accelerometer data yielded confusing results. The auto and cross spectral power densities of the input (input chirp signal) and output (accelerometer readings) for each of the 25 test iterations were averaged to help reduce the noise in the FRFs. The averaged FRFs, however, had no resonant natural frequency peaks – which was unexpected (Fig. 13). Preflight test results predicted resonances around 60, 250, and 660 Hz.[5] Therefore, an anomaly investigation began.

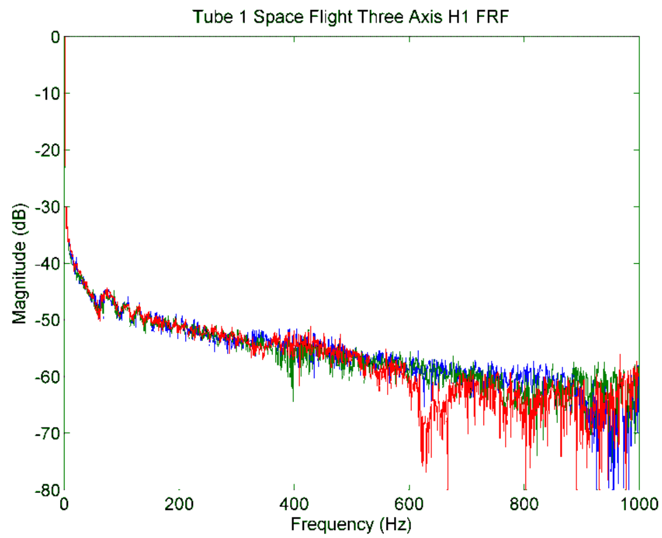

Fig. 13 On-orbit vibration response test *x*, *y*, and *z*-axis H1 0-1000Hz FRF.

The initial investigation questioned the actual sampling rate of the flight computer, however, a sample test indicated the flight computer was performing at the advertised 5000 Hz rate. The anomaly investigation then turned to the input signal and architecture. The input signal was sent from the computer through the digital to analog converter and then through a filter which attenuated frequencies above 1000 Hz, effectively halving the bandwidth of the input chirp signal. Design limitations prevented recording the actual input signal seen by the piezoelectric patches, so a theoretical signal was developed within MATLAB® and then used within the analysis code. At this point a fortuitous error was introduced into the analysis code that generated the FRFs. The error resulted in presentation of the 25th iteration FRF as the averaged FRF – and resonance peaks were present. After the code error was corrected, however, the resonance peaks disappeared (Fig. 11). Stepping backward from the averaging process, each iteration of the vibration response test was analyzed separately, and all had resonance peaks, although they didn't appear to at a consistent frequency. Given the frequency variability, the next step was to present the 25 individual FRFs on the same plot. Figs. 14, 15, and 16 are the final test iteration *x*-axis FRFs for tubes 1-3, and Figs. 17, 18, and 19 are the 25 individual *x*-axis FRFs for tubes 1-3, plotted by iteration rather than amplitude. Figs. 17, 18, and 19 are top views of 3D plots of the 25 FRFs, with the color scheme representing amplitude to clearly highlight the resonance peaks (dark orange). As the figures indicate, the resonance frequencies exhibited time dependency during the space flight vibration response test. The initial analysis efforts' averaging process had therefore washed out the resonant peaks in the averaged FRF because the peaks appear to be uncorrelated from an averaging sense.

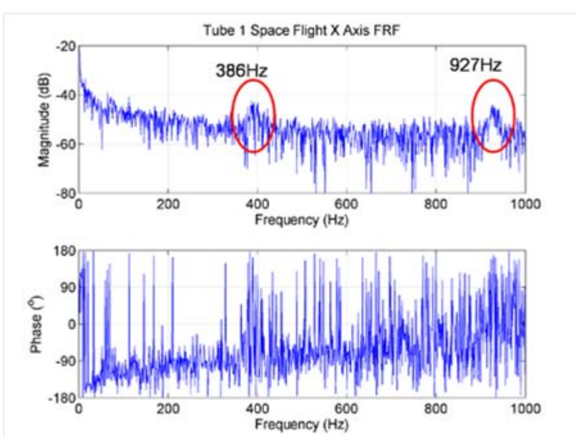

Fig. 14 Tube 1 *x*-axis 0-1000 Hz H1 FRF.

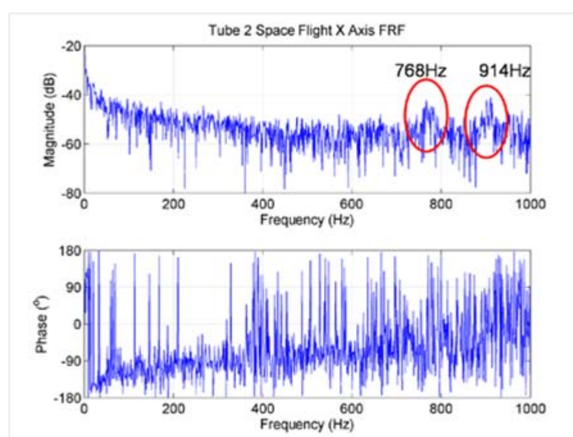

Fig. 15 Tube 2 *x*-axis 0-1000 Hz H1 FRF.

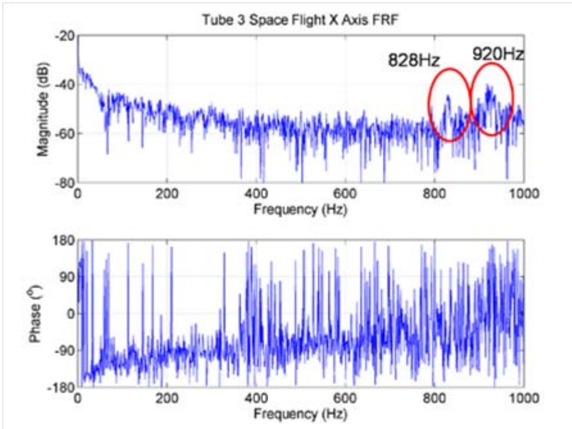

Fig. 16 Tube 3 *x*-axis 0-1000 Hz H1 FRF.

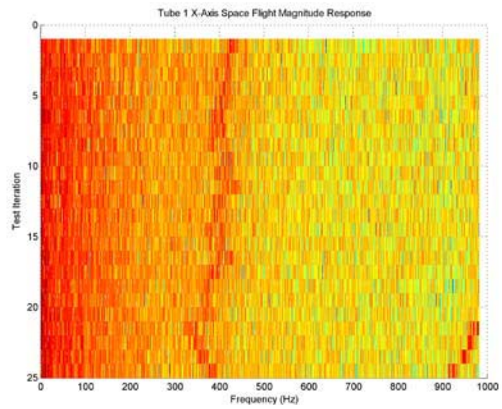

Fig. 17 Tube 1 *x*-axis 01-1000 Hz H1 FRF demonstrating resonance peak drift.

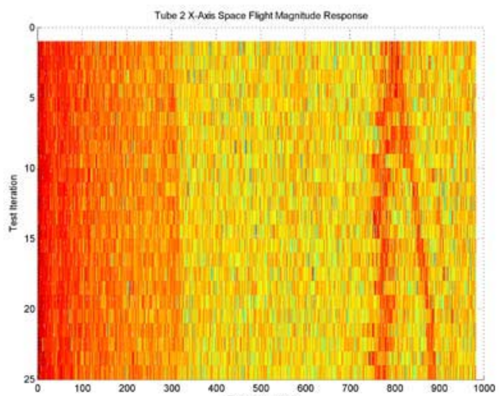

Fig. 18 Tube 2 *x*-axis 01-1000 Hz H1 FRF demonstrating resonance peak drift.

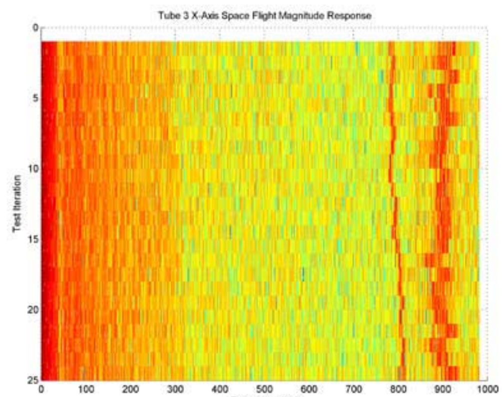

Fig. 19 Tube 3 *x*-axis 01-1000 Hz H1 FRF demonstrating resonance peak drift.

With the answer to the lack of peaks in the averaged space flight FRFs, the next question was simple: why do the peaks drift? The analysis efforts up this point had been based on the assumption of a linear and time invariant system, but Figs. 17, 18, and 19 suggest the tubes were indeed demonstrating time dependence which had not been seen before. No definite answer can be given as to why the tubes in space exhibited time dependency not observed in ground testing, but there are two possible explanations that center on the rigidity and temperature of the tube at the time of testing.

The first possible explanation focuses on the overall temperature and rigidity of the tube itself. If the tube had not cooled enough to sufficiently rigidize during the five minute hold prior to the vibration tests, the structural characteristics would still be changing while the tests were being conducted, yielding time varying structural natural frequencies. Although this theory cannot be proven (the temperature of the tubes at the start of the vibration response testing was not recorded), there is contrary evidence which suggests this should not have happened. In preflight thermal vacuum (TVac) ground testing at chamber temperatures around 25°C, a boom was heated to approximately 165°C and cooled to 100°C (well below glass transition) in 150 seconds[5]; the flight tubes maximum relative ambient structural temperature was approximately 0°C, and the tubes were only heated to 145°C, so the flight tubes' temperature should have been significantly below glass transition by five minutes. One possible explanation is the tubes were covered in Kapton tape which could have caused them to cool at a slower rate than in ground TVac testing. And even if the tube was still very warm, another preflight test indicated increased temperature has no dramatic effect on the structural behavior of the tubes up to 100°C.[6]

The second possible explanation suggests the MFCs changed the flight tubes' structural characteristics by slightly deforming the tube bases via the application of the input bending moment on a still warm (and perhaps pliable) tube surface. The MFCs are epoxied to the tube near the basecap, and remain inside of the oven box after the tube has deployed. It is possible the oven insulation prevented the lower portion of the tube from cooling as rapidly as preflight ground testing suggested, which may have left the base slightly flexible during vibration testing.

The MFCs could conceivably deform the semi-rigid tubes, causing their structural properties to change over time. Again, the temperature of the base of the tube was not recorded at the start of the vibration response testing, but the post-deployment image of flight tube 3 indicates the oven doors had closed after deployment (flight tubes 1 and 2 oven doors remained open). The closed oven doors would trap more heat and thus flight tube 3 should then exhibit the greatest peak drift, however Fig. 19 does not support this conclusion.

C. Post Flight

Concern about any potential hazards that could occur during shipping from Kennedy Space Center to AFIT, the recorded experiment data was copied from the flight computer and several pictures were taken of the successfully deployed tubes. Upon return to AFIT, the first task was to perform a 3D scan with AFIT's FARO Arm.

Three-dimensional location measurements were taken of the camera, bay walls, tube top end cap, and the boom for all three bays. The carbon fiber tube could only be measured from the tube tip through the top of the oven, as the oven prevented the probe from going any lower. While performing contact measurements along the length of the tube, care was taken to not move the tube with the hard probe – doing so would lower the accuracy of the hard probe measurements. Geometric planes were fit to the 3D bay wall and camera point clouds, cylinders were fit to the tubes and top end caps, with another plane fit to the top of the end cap (see Fig. 20).

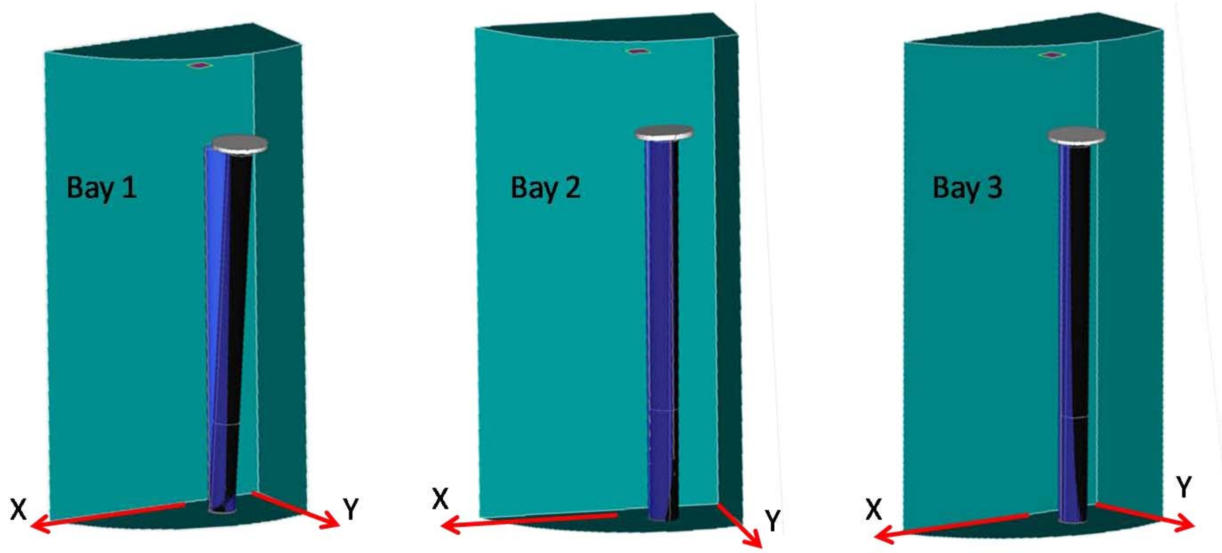

Fig. 20 Measured deployment of each tube (black) overlaid on a true deployment (blue).

The three geometry files (one per bay) were imported into a CAD package for further processing. A linear extrapolation of the cylinder fit to each boom was extended to the floor of the bay to complete the model of the deployed tubes. Using the as-built drawings,[7] a perfectly straight deployed boom was then modeled, centered on the exact location of the tube mount for comparison purposes. First, the horizontal planar *x*- and *y*-axis differences between the perfect and actual deployed tube were measured; this, in essence, is the deviation from true or perfectly straight. Only the horizontal plane deviation calculations were conducted. The vertical differences were not measured due to the influence of potential manufacturing defects and the creases remaining from the major folds would increase the order of uncertainty beyond the error measurements themselves. The intersection of the modeled and actual deployed tubes with the floor of the bay lines up very well for all three bays; the deviation at the bottom between true and deployed is the genesis of the order of error in the horizontal plane deviation measurements.

Fig. 20 shows the finished geometry models. The perfectly deployed tubes are represented with blue cylinders, and the actual deployed tubes are shown with representative black tubes a silver top flange (similar to the carbon fiber and aluminum endcap). Table 2 lists the measured CAD deviations from straight and the results of the image change analysis discussed previously. The CAD analysis shows the deviation from straight post-flight. The image change analysis measures the change from in-space deployed position to post-flight at AFIT deployed position caused by landing, Shuttle removal, shipping, etc. Combining these two measurements yields the deployment deviation from straight *on-orbit*, and is reported in Table 2.

Table 2 CAD, Image Analysis, and True Deployment Error Dimensions (cm).

Tube 1	CAD Analysis	*x* error: -2.90	*y* error: 0.84
	Image Analysis	*x* change: 0.0861	*y* change: -0.9190
	On-Orbit Deviation	*-2.97 cm*	*1.85 cm*
Tube 2	CAD Analysis	*x* error: -0.988	*y* error: -1.244
	Image Analysis	*x* change: unknown	*y* change: unknown
	On-Orbit Deviation	unknown	unknown
Tube 3	CAD Analysis	*x* error: 0.150	*y* error: 0.533
	Image Analysis	*x* change: w/in noise	*y* change: 0.7203
	On-Orbit Deviation	*w/in noise*	*0.18 cm*

As expected, tube 1 shows the largest error as a result of the delayed inflation. The on-orbit deviation of tube 2 is indeterminable (because of a lack of post-flight image for change detection), but the on-orbit deviation of tube 3 was virtually zero – meaning it deployed almost perfectly true on orbit. This is excellent evidence that precision on-orbit deployment is feasible with these sub glass transition inflatable/rigidizable tubes.

The scanning laser vibrometer test results round out the post flight analysis. The 0-500Hz FRFs are shown in Figs. 21, 22, and 23 for tubes 1, 2, and 3, and Fig. 24 presents operating deflection shapes for tube 1. Figs. 21-23 each contain four respective FRFs, which correspond to different scan point on each tube. The presented scan points are arranged vertically on the respective tube, such that the response of the scan point near the bottom of the tube is presented with response of the scan point near the top of the tube, and then two other scan points along the tube. In the operating deflection shape montage, all of the scan points are presented and overlaid on the target tube to present a magnified picture of the deflection shape of the scanned area.

The first resonant natural frequency observed in the post flight testing that correlates with the on-orbit data is the second cantilevered bending mode (373 Hz in Fig. 21, shape B in Fig. 24), which matches fairly well with the observed 386 Hz mode in Fig. 14. Tube 2 has a correlation at 768 Hz, but this correlation is not observable in the 0-500 Hz FRFs presented. Also, note tube 2 has a resonance at 214 Hz – this is a cantilevered torsion mode, which was not readily identified in tubes 1 and 3, and tube 2 has a strong split in the first cantilevered bending mode. Curiously, tube 2 has a stiffer (higher natural frequency) first bending mode (for the split peaks) than tube 3, but tube 3 has a significantly stiffer second cantilevered bending mode (with tip mass). The resonant frequencies and operating deflection shape comments are provided in Table 3.

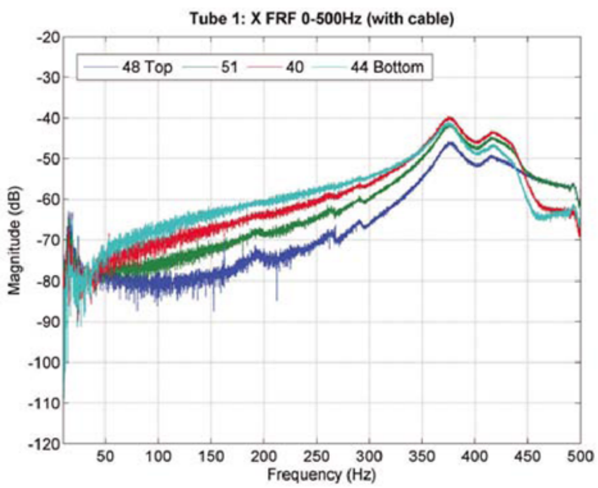

Fig. 21 Tube 1 four 0-500Hz *x*-Axis FRFs.

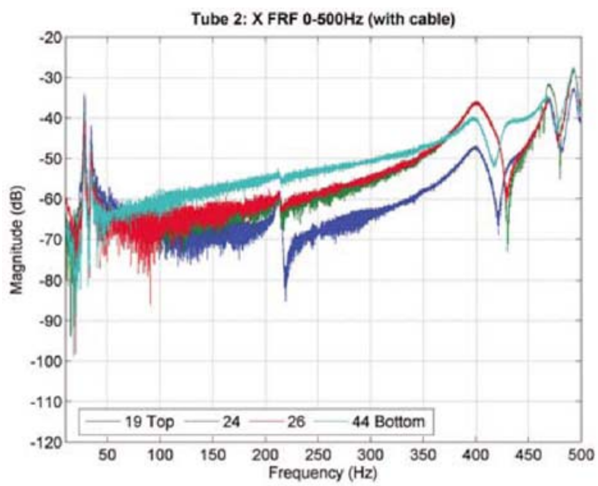

Fig. 22 Tube 2 four 0-500Hz *x*-Axis FRFs.

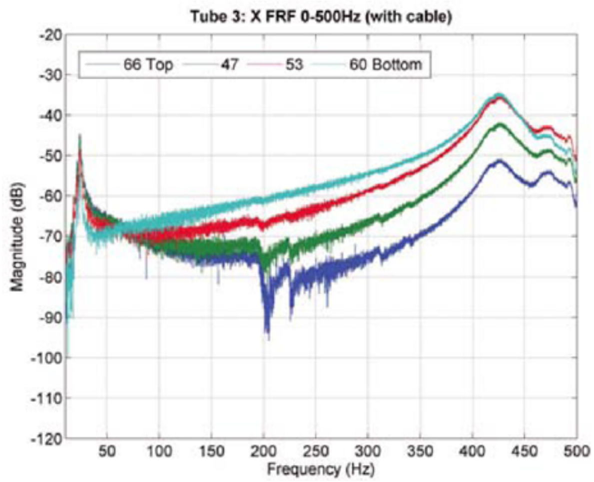

Fig. 23 Tube 3 four 0-500Hz *x*-Axis FRFs.

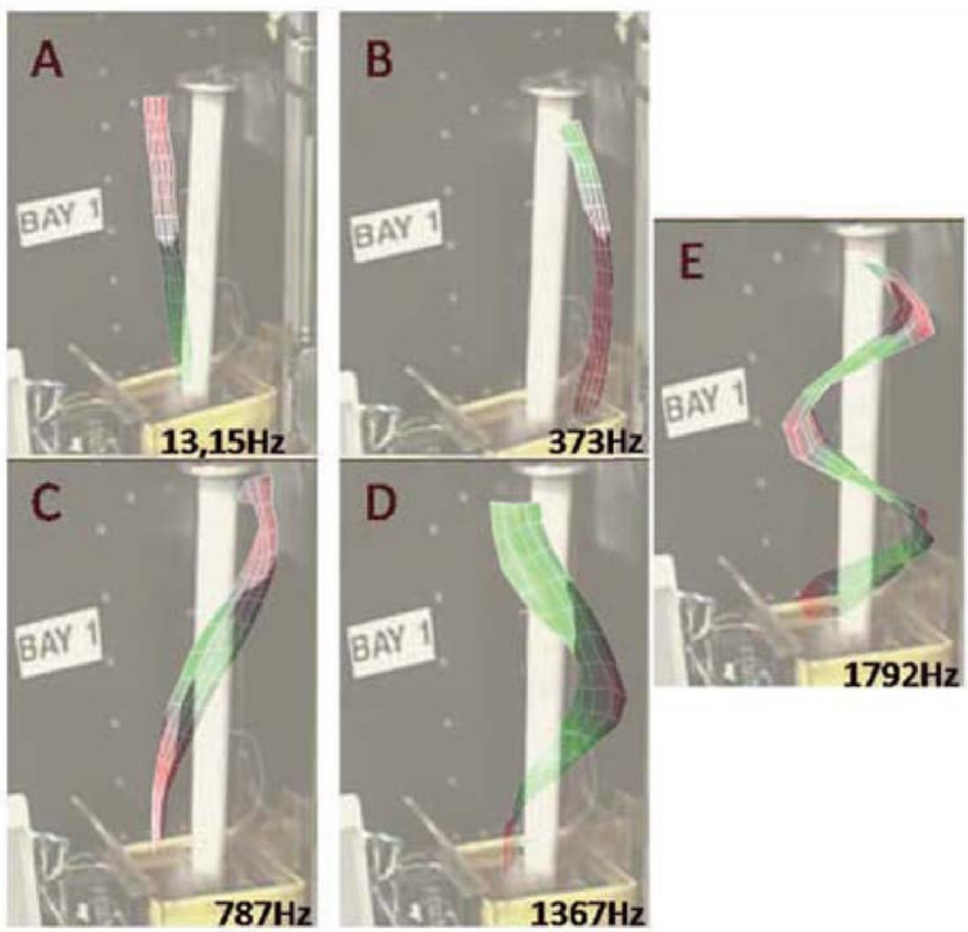

Fig. 24 Tube 1 operating deflection shapes and natural frequencies.

Table 3 Resonant Natural Frequencies and Operating Deflection Shapes from Laser Vibrometer

	Resonance	Natural Frequency (Hz)	Operating Deflection Shape Comments
Tube 1	1	13, 15	First Cantilevered Bending
	2	373	Second Cantilevered Bending with tip mass
	3	787	Second Cantilevered Bending with tip mass and torsion
	6	1792	Fourth Cantilevered Bending
Tube 2	1	28.4, 34.3	First Cantilevered Bending
	2	214	First Cantilievered Torsion
	3	400	Second Cantilevered Bending with tip mass
	4	468,493	Second Cantilevered Bending with tip mass and Torsion
	5	765	Second Pinned-Pinned with Breathing
	9	1690	Fourth Cantilevered Bending
Tube 3	1	23.9	First Cantilevered Bending
	2	426	Second Cantilevered Bending with tip mass
	3	731	Second Cantilevered Bending with tip mass and Torsion
	4	1202	Third Cantilevered Bending with tip mass and Torsion
	6	1441	Fourth Cantilevered Bending with tip mass and Torsion

V. Conclusions

RIGEX completed all of its experimental objectives by successfully inflating and rigidizing carbon fiber composite booms in space. Temperature, pressure, image, and accelerometer data were all successfully collected on-orbit and retrieved for processing. The data shows the ovens performed flawlessly and appear as though they could be reused, important information for consideration in deploying multiple booms on-orbit. The ovens increased the experiment structure temperature significantly, and the structure appeared to be headed toward thermal equilibrium in space. However, in the future thermal control will need to be a more integral part of the design process, particularly for the flight computer.

Boom 3 inflated immediately after the inflation solenoid was commanded open, but tube 2 had a 0.068 second delay, and boom 1 did not inflate while the inflation pressure was being monitored (first five seconds), but is believed to have inflated within 50 seconds of the commanded inflation. Also, recorded on-orbit inflation pressure spikes were correlated to opening pressure seals created by folds in the stowed booms.

The imaging system worked as advertised on-orbit, and through a combination of image change detection analysis and high resolution contact measurement, the exact on-orbit deployment error of boom 1 was determined to be -2.87 and 1.85 cm in the respective *x*- and *y*-axis. Boom 3 achieving an almost perfectly straight deployment on-orbit (within measurement noise and 0.18 cm for *x*- and *y*-axis, respectively) – critical information for precision inflatable deployment necessary for joining large structures on-orbit.

The flight booms exhibited lower natural frequencies on-orbit than were measured in the preflight tests on the ground. During the space flight vibration testing, the resonant frequencies drifted, showing time dependent behavior which was not expected. The flight vibration response test results consist of a few peaks which mostly correlated to post flight vibration response tests. Overall, the first and second bending modes of all three flight tubes and the first torsional mode of flight tube 2 were comparable (but typically at lower frequencies) to the preflight testing modes. The MFC patches used for excitation performed flawlessly in space.

Overall, the RIGEX achieved all of its objectives and generated new avenues for scientific inquiry. It was a successful proof-of-concept demonstration, and results in a TRL increase of inflatable/rigidizable technology for space applications.

Acknowledgments

The authors would like to thank Mr. Jay Anderson, Mr. Wilbur Lacy, and Mr. Sean Miller of AFIT for their technical support, and Capt. Cole Doupe and Capt. Chester McFarland of AFIT for their testing and programming assistance. The authors would also like to thank Dr. Greg Agnes of the Jet Propulsion Laboratory and Dr. Keates Wilkey of NASA Langley for their commitment. RIGEX was integrated and flown under the direction of the Department of Defense's Space Test Program.

References

[1]Jenkins, C.M.H., ed., *Gossamer Spacecraft: Membrane and Inflatable Structures Technology for Space Applications*, Progress in Astronautics and Aeronautics, Vol. 191, AIAA, Reston, VA, ISBN 1563474034, 2001.

[2]Wertz and Larson, *Space Mission Analysis and Design*, Third Edition, Microcosm Press, ISBN 1-881883-10-8, 1999.

[3]Bigelow Aerospace Inflatable Habitats, online at: www.bigelowaerospace.com.

[4]Philley Jr., T.L., *Development, Fabrication, and Ground Test of an Inflatable Structure Space-Flight Experiment*, MS Thesis, Air Force Institute of Technology, Wright-Patterson AFB, OH, 2003.

[5]Moeller, C.R., *Design and Ground-Testing of an Inflatable-Rigidizable Structure Experiment in Preparation for Space Flight*, MS Thesis, Air Force Institute of Technology, Wright-Patterson AFB, OH, 2005.

[6]Single, *Experimental Vibration Analysis of Inflatable Beams for an AFIT Experiment*, MS Thesis, Air Force Institute of Technology, Wright-Patterson AFB, OH, 2002.

[7]Owens, J.J., *Final Assembly, Testing and Processing of the Rigidizable Inflatable Get-Away-Special Experiment (RIGEX) for Spaceflight Qualification*, MS Thesis, Air Force Institute of Technology, Wright-Patterson AFB, OH, 2007.